



Cite this: *Dalton Trans.*, 2015, **44**, 7626

$[\text{Cu}(\text{N}^{\wedge}\text{N})(\text{P}^{\wedge}\text{P})]^+$ complexes with 2,2':6',2''-terpyridine ligands as the $\text{N}^{\wedge}\text{N}$ domain†

Niamh S. Murray, Sarah Keller, Edwin C. Constable, Catherine E. Housecroft,*
Markus Neuburger and Alessandro Prescimone

The first examples of $[\text{Cu}(\text{N}^{\wedge}\text{N})(\text{POP})]^+$ complexes (POP = bis(2-(diphenylphosphino)phenyl)ether) in which the $\text{N}^{\wedge}\text{N}$ domain is a 2,2':6',2''-terpyridine (tpy) ligand have been prepared and characterized; $\text{N}^{\wedge}\text{N}$ = tpy, 5,5''-dimethyl-2,2':6',2''-terpyridine (**1**), 4'-(4-tolyl)-2,2':6',2''-terpyridine (**2**), 4'-(4-*n*-propoxyphenyl)-2,2':6',2''-terpyridine (**3**) and 4'-(4-*n*-butoxyphenyl)-2,2':6',2''-terpyridine (**4**). In solution, the tpy domain in each $[\text{Cu}(\text{N}^{\wedge}\text{N})(\text{POP})][\text{PF}_6]$ complex is C_2 -symmetric, consistent with either tridentate coordination or a low energy dynamic process involving bidentate ligands; for $[\text{Cu}(\textbf{2})(\text{POP})][\text{PF}_6]$ and $[\text{Cu}(\textbf{4})(\text{POP})][\text{PF}_6]$, the ^1H NMR spectra showed negligible change between 295 and 210 K. The single crystal structures of $[\text{Cu}(\text{tpy})(\text{POP})][\text{PF}_6]$ and $[\text{Cu}(\textbf{4})(\text{POP})][\text{PF}_6]$ are presented. The asymmetric unit of $[\text{Cu}(\text{tpy})(\text{POP})][\text{PF}_6]$ contains two independent cations; in one the tpy ligand is tridentate and in the other, it is bidentate with the non-coordinated pyridine ring facing the Cu atom ($\text{Cu}\cdots\text{N} = 3.146(1) \text{ \AA}$). In contrast, the solid-state structure of $[\text{Cu}(\textbf{4})(\text{POP})][\text{PF}_6]$ features a $[\text{Cu}(\textbf{4})(\text{POP})]^+$ cation containing a bidentate tpy-domain with the non-coordinated pyridine ring oriented with the N-atom facing away from the Cu atom; this conformation may be associated with inter-cation $\text{N}\cdots\text{HC}$ non-classical hydrogen bonds. The photo-physical properties of $[\text{Cu}(\text{N}^{\wedge}\text{N})(\text{POP})][\text{PF}_6]$ with $\text{N}^{\wedge}\text{N}$ = tpy or **1–4** are described. In the solid state at room temperature, the compounds are poorly emissive. In solution, the emission behaviour is consistent with ligand dissociation. This is supported by ^1H and ^{31}P NMR spectroscopic data which show POP and $[\text{Cu}(\text{POP})_2]^+$ in solutions of aged samples; mass spectrometric data are consistent with the formation of $[\text{Cu}(\text{N}^{\wedge}\text{N})_2]^{2+}$ in these samples.

Received 4th February 2015,

Accepted 19th March 2015

DOI: 10.1039/c5dt00517e

www.rsc.org/dalton

Introduction

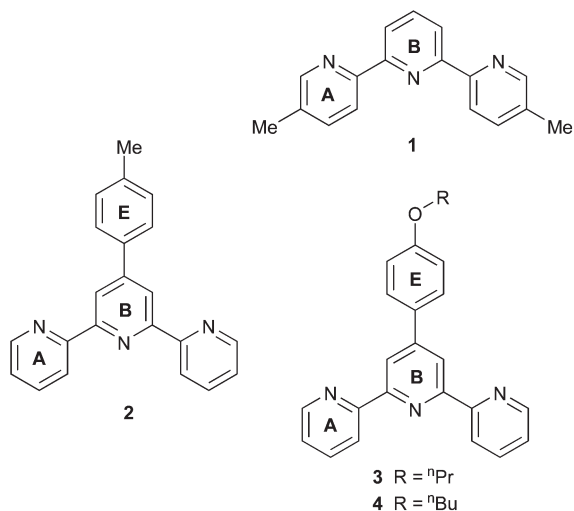
Light-emitting electrochemical cells (LECs) are a developing technology in solid-state lighting and, in common with organic light-emitting diodes (OLEDs), offer increased energy savings when compared to traditional white-light sources.¹ LECs possess a simpler device architecture than OLEDs and are assembled using solution, rather than vacuum, processing. Typically, the emissive layer in a LEC is a conjugated light-emitting polymer mixed with an ionic iridium(III) or ruthenium(II) complex.¹ However, a future with sustainable energy encourages the use of Earth-abundant metals in place of rare platinum group metals. Copper(I)-based complexes of the type $[\text{Cu}(\text{N}^{\wedge}\text{N})(\text{P}^{\wedge}\text{P})]^+$ or $[\text{Cu}(\text{P}^{\wedge}\text{P})_2]^+$ ($\text{N}^{\wedge}\text{N}$ and $\text{P}^{\wedge}\text{P}$ = chelating ligands) are encouraging contenders for applications in

LECs.^{2–6} Emission is improved by incorporating sterically demanding $\text{P}^{\wedge}\text{P}$ ligands¹ and two popular choices are bis(2-(diphenylphosphino)phenyl)ether (POP) and 4,5-bis(diphenylphosphino)-9,9-dimethylxanthene (xantphos).^{2,6–14}

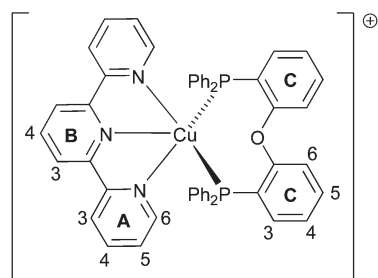
The most commonly employed $\text{N}^{\wedge}\text{N}$ chelates in $[\text{Cu}(\text{N}^{\wedge}\text{N})(\text{P}^{\wedge}\text{P})]^+$ complexes are those based on 2,2'-bipyridine (bpy) or 1,10-phenanthroline (phen). Recently, we demonstrated that 2,2':6',2''-terpyridines bind to iridium(III) in a bidentate mode in octahedral $[\text{Ir}(\text{C}^{\wedge}\text{N})_2(\text{N}^{\wedge}\text{N})]^+$ ($\text{C}^{\wedge}\text{N}$ = cyclometallated ligand) complexes. These complex cations were successfully employed in LECs which displayed rapid turn-on times, although their efficiencies were relatively low.¹⁵ We were therefore encouraged to investigate the use of 2,2':6',2''-terpyridine (tpy) ligands in $[\text{Cu}(\text{tpy})(\text{P}^{\wedge}\text{P})]^+$ complexes. By using a Kröhnke¹⁶ or one-pot method,¹⁷ it is straightforward to synthesize a range of 4'-functionalized tpy ligands (4'-Xtpy), and thereby tune the electronic properties of $[\text{Cu}(4'\text{-Xtpy})(\text{POP})]^+$. To the best of our knowledge, no $[\text{Cu}(\text{tpy})(\text{P}^{\wedge}\text{P})]^+$ complexes have previously been described, although a handful of related $[\text{Cu}(\text{tpy})(\text{PPh}_3)_2]^+$ complexes have been structurally characterized.^{18–20} In $[\text{Cu}(\text{tpy})(\text{PPh}_3)_2][\text{ClO}_4]$,¹⁸ and $[\text{Cu}(4'\text{-Phtpy})(\text{PPh}_3)_2][\text{BF}_4]$ ¹⁹ (4'-Phtpy = 4'-phenyl-2,2':6',2''-terpyridine), the tpy ligand is tridentate and the

Department of Chemistry, University of Basel, Spitalstrasse 51, CH-4056 Basel, Switzerland. E-mail: catherine.housecroft@unibas.ch

†Electronic supplementary information (ESI) available: Fig. S1. VT ^1H NMR spectra of $[\text{Cu}(\textbf{4})(\text{POP})][\text{PF}_6]$; Fig. S2. ^{31}P NMR spectra of aged samples of $[\text{Cu}(\text{N}^{\wedge}\text{N})(\text{POP})][\text{PF}_6]$ ($\text{N}^{\wedge}\text{N}$ = tpy, **1–4**). CCDC 1041066 and 1041067. For ESI and crystallographic data in CIF or other electronic format see DOI: 10.1039/c5dt00517e



Scheme 1 Structures of ligands 1–4; ring labelling for NMR spectroscopic assignments, see also Scheme 2.



Scheme 2 Schematic structure of $[\text{Cu}(\text{tpy})(\text{POP})]^+$ with atom labelling for NMR spectroscopic assignments. In the PPH_2 units, the Ph rings are labelled D. See also Scheme 1 for ring labels.

copper(i) centre is in a distorted trigonal bipyramidal environment. In contrast, in $[\text{Cu}\{4'-(2\text{-Br-5-py})\text{tpy}\}(\text{PPh}_3)_2][\text{BF}_4]$ ($4'-(2\text{-Br-5-py})\text{tpy} = 4'-(2\text{-bromo-5-pyridyl-2,2':6',2''-terpyridine})$, the tpy domain acts as an N^3N chelate.²⁰ We now report the syntheses and properties of $[\text{Cu}(\text{tpy})(\text{POP})][\text{PF}_6]$ and four of its derivatives containing ligands 1–4 (Scheme 1).

Experimental

General

^1H , $^{13}\text{C}\{^1\text{H}\}$ and $^{31}\text{P}\{^1\text{H}\}$ NMR spectra were recorded on a Bruker Avance III-500 NMR spectrometer (chemical shifts with respect to $\delta(\text{TMS}) = 0$ ppm for ^1H and ^{13}C , and 85% aqueous H_3PO_4 for ^{31}P). Solution electronic absorption and emission spectra were recorded on an Agilent 8453 spectrophotometer and Shimadzu 5301PC spectrofluorophotometer, respectively. Electrospray ionization (ESI) mass spectra were recorded on a Bruker esquire 3000^{plus} mass spectrometer. Solution and solid-state quantum yields were measured using a Hamamatsu

absolute PL quantum yield spectrometer C11347 Quantaaurus_QY. Lifetimes and emission spectra of powdered samples were measured using a Hamamatsu Compact Fluorescence lifetime Spectrometer C11367 Quantaaurus-Tau; an LED light source with excitation wavelength of 365 nm was used.

The compounds tpy,²¹ 1,^{21,22} 2,²³ 3²⁴ and 4²⁴ and $[\text{Cu}(\text{MeCN})_4][\text{PF}_6]^{25}$ were prepared as previously reported. All other chemicals were used as received.

$[\text{Cu}(\text{tpy})(\text{POP})][\text{PF}_6]$. A colourless solution of $[\text{Cu}(\text{MeCN})_4][\text{PF}_6]$ (56 mg, 0.15 mmol) and POP (81 mg, 0.15 mmol) in CH_2Cl_2 (30 mL) was stirred for 2 h. Then tpy (35 mg, 0.15 mmol) was added causing a colour change to yellow; the solution was stirred for 2 h. The solution was filtered, all volatiles were removed *in vacuo* and the yellow residue was washed with hexane (5×5 mL). $[\text{Cu}(\text{tpy})(\text{POP})][\text{PF}_6]$ was isolated as a yellow powder (156 mg, 0.14 mmol, 95%). ^1H NMR (500 MHz, CD_2Cl_2 , 295 K) δ/ppm 8.19 (dd, $J = 5.2, 1.9$ Hz, 2H, H^{A6}), 8.07 (m, 1H, H^{B4}), 8.01 (m, 2H, H^{B3}), 7.80 (d, $J = 7.9$ Hz, 2H, H^{A3}), 7.62 (td, $J = 7.8, 1.8$ Hz, 2H, H^{A4}), 7.27 (m, 6H, $\text{H}^{\text{C5+D4}}$), 7.10–7.02 (overlapping m, 12H, $\text{H}^{\text{C4+D3+A5}}$), 6.96 (m, 2H, H^{C6}), 6.87 (m, 2H, H^{C3}), 6.83 (m, 8H, H^{D2}). $^{13}\text{C}\{^1\text{H}\}$ NMR (126 MHz, CD_2Cl_2 , 295 K) δ/ppm 158.2 (t, $J_{\text{PC}} = 6.0$ Hz, C^{C1}), 155.7 (C^{B2}), 154.7 (C^{A2}), 149.9 (C^{A6}), 139.5 (C^{B4}), 138.3 (C^{A4}), 134.7 (C^{C3}), 133.7 (t, $J_{\text{PC}} = 8.0$ Hz, C^{D2}), 132.5 (C^{C5}), 131.6 (t, $J_{\text{PC}} = 16.0$ Hz, C^{D1}), 130.3 (C^{D4}), 129.0 ($J_{\text{PC}} = 4.5$ Hz, C^{D3}), 125.6 (overlapping $\text{C}^{\text{C2+C4}}$), 125.4 (C^{A5}), 124.6 (C^{B3}), 123.3 (C^{A3}), 120.4 (C^{C6}). $^{31}\text{P}\{^1\text{H}\}$ NMR (162 MHz, CD_2Cl_2 , 295 K) δ/ppm –12.5 (broad, FWHM = 420 Hz, POP), –144.5 (septet, $J_{\text{PF}} = 710$ Hz, $[\text{PF}_6]^-$). UV-Vis (CH_2Cl_2 , 2.5×10^{-5} mol dm^{-3}): λ/nm ($\epsilon/\text{dm}^3 \text{mol}^{-1} \text{cm}^{-1}$) 229 (46 200), 273 sh (22 300), 300 sh (19 000), 392 (2600). ESI MS: m/z 834.5 $[\text{M} - \text{PF}_6]^+$ (calc. 834.2), 601.4 $[\text{M} - \text{PF}_6 - \text{tpy}]^+$ (base peak, calc. 601.1). Found C 62.48 H 4.41, N 4.47; $\text{C}_{51}\text{H}_{39}\text{CuF}_6\text{N}_3\text{OP}_3$ requires C 62.48, H 4.01, N 4.29%.

$[\text{Cu}(\text{1})(\text{POP})][\text{PF}_6]$. A colourless solution of $[\text{Cu}(\text{MeCN})_4][\text{PF}_6]$ (93 mg, 0.25 mmol) and POP (134 mg, 0.25 mmol) in CH_2Cl_2 (40 mL) was stirred for 2 h. Compound 1 (88 mg, 0.25 mmol) was added; the now yellow solution was stirred for 4 h. Solvent was removed *in vacuo*; the yellow residue was dissolved in CH_2Cl_2 (4 mL) and the solution layered with Et_2O . $[\text{Cu}(\text{1})(\text{POP})][\text{PF}_6]$ precipitated and was isolated as a yellow powder (211 mg, 0.24 mmol, 95%). ^1H NMR (500 MHz, CD_2Cl_2) δ/ppm 8.02 (m, 1H, H^{B4}), 7.99 (d, $J = 2.1$ Hz, 2H, H^{A6}), 7.93 (m, 2H, H^{B3}), 7.65 (d, $J = 8.1$ Hz, H^{A3}), 7.40 (dd, $J = 8.1, 1.5$ Hz, H^{A4}), 7.26 (m, 6H, $\text{H}^{\text{D4+C5}}$), 7.08 (m, 8H, H^{D3}), 7.03 (td, $J = 7.6, 1.1$ Hz, H^{C4}), 6.95 (m, 2H, H^{C6}), 6.85 (m, 10H, $\text{H}^{\text{C3+D2}}$), 2.04 (s, 6H, H^{Me}). $^{13}\text{C}\{^1\text{H}\}$ NMR (126 MHz, CD_2Cl_2) δ/ppm 158.2 ($J_{\text{PC}} = 5.9$ Hz, C^{C1}), 155.8 (C^{B2}), 152.1 (C^{A2}), 150.5 (C^{A6}), 139.3 (C^{B4}), 138.5 (C^{A4}), 135.7 (C^{A5}), 134.7 (C^{C3}), 133.9 (t, $J = 8.0$ Hz, C^{D2}), 132.4 (C^{C5}), 131.6 (t, $J = 16.0$ Hz, C^{D1}), 130.3 (C^{D4}), 128.9 (t, $J = 4.4$ Hz, C^{D3}), 125.6 (overlapping, $\text{C}^{\text{C4+C2}}$), 123.9 (C^{B3}), 122.7 (C^{A3}), 120.2 (C^{C6}), 18.7 (C^{Me}). $^{31}\text{P}\{^1\text{H}\}$ NMR (202 MHz, CD_2Cl_2) δ/ppm –12.1 (broad, FWHM = 310 Hz, POP), –144.5 (septet, $J_{\text{PF}} = 710$ Hz, $[\text{PF}_6]^-$). UV-Vis (CH_2Cl_2 , 2.5×10^{-5} mol dm^{-3}): λ/nm ($\epsilon/\text{dm}^3 \text{mol}^{-1} \text{cm}^{-1}$) 228 (47 100), 250 sh (31 000), 274 sh (26 800), 306 sh (20 200), 390 (2600). ESI MS: m/z 862.6 $[\text{M} - \text{PF}_6]^+$ (base peak, calc. 862.2). Found C 62.31, H 4.48,



N 4.34; $C_{53}H_{43}CuF_6N_3OP_3 \cdot H_2O$ requires C 62.02, H 4.42, N 4.09%.

[Cu(2)(POP)][PF₆]. A colourless solution of $[Cu(MeCN)_4][PF_6]$ (93 mg, 0.25 mmol) and POP (134 mg, 0.25 mmol) in CH_2Cl_2 (40 mL) was stirred for 2 h. Then **2** (81 mg, 0.25 mmol) was added causing a colour change to yellow. This solution was stirred for 2 h, was then filtered and the solvent removed *in vacuo*. $[Cu(2)(POP)][PF_6]$ was isolated as an orange-yellow powder (180 mg, 0.17 mmol, 67%). ¹H NMR (500 MHz, $CDCl_3$) δ /ppm 8.23 (s, 2H, H^{B3}), 8.21 (overlapping d, $J \approx 5$ Hz, 2H, H^{A6}), 7.99 (d, $J = 7.9$ Hz, 2H, H^{A3}), 7.77 (d, $J = 8.1$ Hz, 2H, H^{E2}), 7.67 (td, $J = 7.8, 1.6$ Hz, 2H, H^{A4}), 7.40 (d, $J = 8.0$ Hz, 2H, H^{E3}), 7.27 (m, 6H, H^{D4+C5}), 7.14–7.07 (m, 10H, H^{A5+D3}), 7.05 (t, $J = 7.5$ Hz, H^{C4}), 6.97 (m, 2H, H^{C6}), 6.85 (m, 10H, H^{C3+D2}), 2.45 (s, 3H, H^{Me}). ¹³C{¹H} NMR (126 MHz, $CDCl_3$) δ /ppm 157.7 (t, $J_{PC} = 6.0$ Hz, C^{C1}), 155.8 (m, C^{B2}), 154.6 (C^{A2}), 151.3 (C^{B4}), 149.3 (C^{A6}), 140.9 (C^{E4}), 138.2 (C^{A4}), 134.4 (C^{C3}), 133.3 (t, $J_{PC} = 7.9$ Hz, C^{D2} overlapping with C^{E1}), 132.1 (C^{C5}), 131.0 (t, $J_{PC} = 16.1$ Hz, C^{D1}), 130.4 (C^{E3}), 130.0 (C^{D4}), 128.7 (t, $J_{PC} = 4.6$ Hz, C^{D3}), 127.3 (C^{E2}), 125.3 (C^{C4}), 125.0 (overlapping, C^{A5+C2}), 123.3 (C^{A3}), 121.7 (C^{B3}), 119.9 (C^{C6}), 21.5 (C^{Me}). ³¹P{¹H} NMR (162 MHz, $CDCl_3$) δ /ppm –12.4 (broad, FWHM = 100 Hz, POP), –144.2 (septet, $J_{PF} = 713$ Hz, $[PF_6]^-$). UV-Vis (CH_2Cl_2 , 2.5×10^{-5} mol dm⁻³): λ /nm (ϵ /dm³ mol⁻¹ cm⁻¹) 229 (51 200), 282 (40 600), 398 (3900). ESI MS: m/z 924.6 $[M - PF_6]^+$ (base peak, calc. 924.2). Found C 64.18, H 4.45, N 4.07; $C_{58}H_{45}CuF_6N_3OP_3 \cdot H_2O$ requires C 64.00, H 4.35, N 3.86%.

[Cu(3)(POP)][PF₆]. A colourless solution of $[Cu(MeCN)_4][PF_6]$ (93 mg, 0.25 mmol) and POP (134 mg, 0.25 mmol) in CH_2Cl_2 (40 mL) was stirred for 2 h. Then **4** (92 mg, 0.25 mmol) was added to give a yellow solution that was stirred for 4 h. Solvent was removed *in vacuo*; the yellow residue was dissolved in CH_2Cl_2 (4 mL) and the solution layered with Et₂O. This yielded $[Cu(4)(POP)][PF_6]$ as a yellow precipitate which was collected by filtration (264 mg, 0.24 mmol, 95%). ¹H NMR (500 MHz, CD_2Cl_2) δ /ppm 8.22 (d, $J = 4.5$ Hz, 2H, H^{A6}), 8.15 (s, 2H, H^{B3}), 7.86 (d, $J = 8.0$ Hz, 2H, H^{A3}), 7.77 (m, 2H, H^{E2}), 7.62 (td, $J = 7.8, 1.8$ Hz, 2H, H^{A4}), 7.26 (m, 6H, H^{D4+C5}), 7.13–7.06 (m, 12H, H^{D3+A5+E3}), 7.03 (t, $J = 7.5$ Hz, 2H, H^{C4}), 6.96 (m, 2H, H^{C6}), 6.84 (m, 10H, H^{C3+D2}), 4.02 (t, $J = 6.6$ Hz, 2H, H^{OCH₂}), 1.85 (m, 2H, H^{OCH₂CH₂}), 1.07 (t, $J = 7.4$ Hz, 2H, H^{Me}). ¹³C{¹H} NMR (126 MHz, CD_2Cl_2) δ /ppm 161.9 (C^{E4}), 158.3 (C^{C1}), 156.2 (C^{B2}), 155.1 (C^{A2}), 149.9 (C^{A6}), 144.7 (C^{B4}), 138.3 (C^{A4}), 134.8 (C^{C3}), 133.8 (t, $J_{PC} = 7.9$ Hz, C^{D2}), 132.5 (C^{C5}), 131.6 (t, $J_{PC} = 15.9$ Hz, C^{D1}), 130.3 (C^{D4}), 129.0 (C^{D3+E2}), 128.7 (C^{E1}), 125.6 (C^{C4}), 125.3 (overlapping, C^{A5+C2}), 123.3 (C^{B3}), 121.7 (C^{A3}), 120.4 (C^{C6}), 115.9 (C^{E3}), 70.4 (C^{OCH₂}), 23.0 (C^{OCH₂CH₂}), 10.7 (C^{Me}). ³¹P{¹H} NMR (202 MHz, CD_2Cl_2) δ /ppm –12.5 (broad, FWHM = 280 Hz, POP), –144.5 (septet, $J_{PF} = 711$ Hz, $[PF_6]^-$). UV-Vis (CH_2Cl_2 , 2.5×10^{-5} mol dm⁻³): λ /nm (ϵ /dm³ mol⁻¹ cm⁻¹) 230 (57 300), 280 (36 900), 315 sh (32 000), 393 (5300). ESI MS: m/z 968.7 $[M - PF_6]^+$ (base peak, calc. 968.3). Found C 62.17, H 4.66, N 3.79; $C_{60}H_{49}CuF_6N_3OP_3 \cdot 2H_2O$ requires C 62.64, H 4.64, N 3.65%.

[Cu(4)(POP)][PF₆]. A colourless solution of $[Cu(MeCN)_4][PF_6]$ (93 mg, 0.25 mmol) and POP (134 mg, 0.25 mmol) in CH_2Cl_2

(40 mL) was stirred for 2 h, and then **5** (95 mg, 0.25 mmol) was added. The yellow solution was stirred for 4 h, after which time the solvent was removed *in vacuo*. The yellow residue was dissolved in CH_2Cl_2 (4 mL) and after an Et₂O layer had been added, the product precipitated. Yellow $[Cu(5)(POP)][PF_6]$ was collected by filtration (242 mg, 0.24 mmol, 96%). ¹H NMR (500 MHz, CD_2Cl_2) δ /ppm 8.22 (d, $J = 4.9$ Hz, 2H, H^{A6}), 8.14 (s, 2H, H^{B3}), 7.86 (d, $J = 8.0$ Hz, 2H, H^{A3}), 7.76 (m, 2H, H^{E2}), 7.62 (td, $J = 7.8, 1.7$ Hz, 2H, H^{A4}), 7.27 (m, 6H, H^{D4+C5}), 7.12–7.06 (m, 12H, H^{D3+A5+E3}), 7.03 (td, $J = 7.5, 1.1$ Hz, 2H, H^{C4}), 6.96 (m, 2H, H^{C6}), 6.84 (m, 10H, H^{C3+D2}), 4.07 (t, $J = 6.5$ Hz, 2H, H^{OCH₂}), 1.81 (m, 2H, H^{OCH₂CH₂}), 1.53 (m, 2H, H^{CH₂Me}), 1.00 (t, $J = 7.4$ Hz, 2H, H^{Me}). ¹³C{¹H} NMR (126 MHz, CD_2Cl_2) δ /ppm 162.0 (C^{E4}), 158.3 (C^{C1}), 156.3 (C^{B2}), 155.4 (C^{A2}), 149.9 (C^{A6}), 138.3 (C^{A4}), 134.7 (C^{C3}), 133.8 (t, $J_{PC} = 8.0$ Hz, C^{D2}), 132.3 (C^{C5}), 131.7 (C^{D1}), 130.3 (C^{D4}), 129.0 (C^{D3+E2}), 128.7 (C^{E1}), 125.9 (C^{C2}), 125.3 (C^{C4}), 125.0 (C^{A5}), 123.2 (C^{A3}), 121.7 (C^{B3}), 120.3 (C^{C6}), 115.9 (C^{E3}), 68.5 (C^{OCH₂}), 31.4 (C^{OCH₂CH₂}), 19.6 (C^{CH₂Me}), 14.0 (C^{Me}), (C^{B4} not resolved). ³¹P{¹H} NMR (162 MHz, CD_2Cl_2) δ /ppm –12.4 (broad, FWHM = 180 Hz, POP), –144.5 (septet, $J_{PF} = 710$ Hz, $[PF_6]^-$). UV-Vis (CH_2Cl_2 , 2.5×10^{-5} mol dm⁻³): λ /nm (ϵ /dm³ mol⁻¹ cm⁻¹) 230 (52 400), 282 (34 600), 316 (30 100), 390 (5300). ESI MS: m/z 982.7 $[M - PF_6]^+$ (base peak, calc. 982.3). Found C 64.70, H 4.81, N 3.79; $C_{61}H_{51}CuF_6N_3OP_3$ requires C 64.92, H 4.56, N 4.02%.

Crystallography

Single crystal data were collected on a Bruker APEX-II diffractometer with data reduction, solution and refinement using the programs APEX²⁶ and CRYSTALS,²⁷ and diagrams and structure analysis used Mercury v. 3.0.1 and v. 3.3.^{28,29}

[Cu(tpy)(POP)][PF₆]. $C_{51}H_{39}CuF_6N_3OP_3$, $M = 980.35$, yellow block, monoclinic, space group $P2_1/n$, $a = 25.8524(15)$, $b = 13.7588(8)$, $c = 27.0506(16)$ Å, $\beta = 111.601(2)^\circ$, $U = 8946.1(9)$ Å³, $Z = 8$, $D_c = 1.456$ Mg m⁻³, $\mu(Cu-K\alpha) = 2.283$ mm⁻¹, $T = 123$ K. Total 90 551 reflections, 16 223 unique, $R_{int} = 0.0231$. Refinement of 15 682 reflections (1235 parameters) with $I > 2\sigma(I)$ converged at final $R_1 = 0.0331$ (R_1 all data = 0.0336), $wR_2 = 0.0352$ (wR_2 all data = 0.0373), $gof = 1.0943$. CCDC 1041066.

[Cu(4)(POP)][PF₆]. $C_{61}H_{51}CuF_6N_3O_2P_3$, $M = 1128.55$, yellow needle, monoclinic, space group $P2_1/n$, $a = 14.5733(12)$, $b = 20.7239(18)$, $c = 18.0544(16)$ Å, $\beta = 105.530(5)^\circ$, $U = 5253.6(5)$ Å³, $Z = 4$, $D_c = 1.427$ Mg m⁻³, $\mu(Cu-K\alpha) = 2.036$ mm⁻¹, $T = 123$ K. Total 31 539 reflections, 9143 unique, $R_{int} = 0.062$. Refinement of 9133 reflections (685 parameters) with $I > 2\sigma(I)$ converged at final $R_1 = 0.0688$ (R_1 all data = 0.0336), $wR_2 = 0.0896$ (wR_2 all data = 0.1962), $gof = 0.9709$. CCDC 1041067.

Results and discussion

Complex synthesis and mass spectrometric and NMR spectroscopic characterization

The complex $[Cu(tpy)(POP)][PF_6]$ was prepared by reaction of $[Cu(MeCN)_4][PF_6]$ with POP followed, after 2 hours, by treatment of the reaction mixture with tpy. This strategy² does not



require the isolation of the intermediate complex $[\text{Cu}(\text{POP})(\text{MeCN})_2]$,³⁰ and avoids competitive formation of homoleptic copper(i) complexes containing *tpy* ligands.³¹ An analogous method was used to prepare $[\text{Cu}(1)(\text{POP})][\text{PF}_6]$, $[\text{Cu}(2)(\text{POP})][\text{PF}_6]$, $[\text{Cu}(3)(\text{POP})][\text{PF}_6]$ and $[\text{Cu}(4)(\text{POP})][\text{PF}_6]$, and the five complexes were isolated as yellow solids in yields ranging from 67–96%. The electrospray mass spectrum of each complex exhibited a peak envelope corresponding to $[\text{M} - \text{PF}_6]^+$ with a characteristic isotope pattern for copper. In the mass spectrum of $[\text{Cu}(\text{tpy})(\text{POP})][\text{PF}_6]$, the base peak corresponded to the $[\text{Cu}(\text{POP})]^+$ ion.

The room temperature solution ^1H and $^{13}\text{C}\{^1\text{H}\}$ NMR spectra of the five complexes were assigned using COSY, HMQC and HMBC methods. In $[\text{Cu}(2)(\text{POP})][\text{PF}_6]$, an HMBC cross peak between H^{Me} and $\text{C}^{\text{E}3}$ (see Scheme 1) distinguished the ^{13}C NMR signals for $\text{C}^{\text{E}3}$ and $\text{C}^{\text{E}2}$. Further confirmation of these assignments comes from the shift for the ^{13}C NMR signal for $\text{C}^{\text{E}3}$ from δ 130.4 ppm in $[\text{Cu}(2)(\text{POP})]^+$ to δ 115.9 ppm in $[\text{Cu}(3)(\text{POP})]^+$ and $[\text{Cu}(4)(\text{POP})]^+$ as the alkoxy substituents are introduced (Scheme 1). The ^1H NMR spectrum of $[\text{Cu}(\text{tpy})(\text{POP})][\text{PF}_6]$ is shown in Fig. 1 and is consistent with a C_2 -symmetric *tpy* domain. This was true for all the complexes. The ^1H NMR spectra of $[\text{Cu}(2)(\text{POP})][\text{PF}_6]$ (Fig. 2, 295 to 220 K) and of $[\text{Cu}(4)(\text{POP})][\text{PF}_6]$ (Fig. S1,[†] 290 to 210 K) were essentially invariant upon cooling, showing only slight shifting of several signals. These data indicate either that the *tpy* domain acts as a tridentate ligand and that the copper(i) centre is 5-coordinate, or that the *tpy* unit is bidentate and undergoes dynamic behaviour on the NMR timescale with a low energy barrier to the process. The C_2 -symmetric *tpy* domain in $[\text{Cu}(4)(\text{POP})]^+$ observed in solution on the NMR timescale contrasts with the solid-state structure discussed below.

Over time, the copper(i) complexes are rather unstable. In the ^1H NMR spectrum of each complex, signals arising from the free POP ligand were observed for aged samples, but no signals for a second *tpy* environment were apparent. In the ^{31}P NMR spectra (Fig. S2[†]), signals for free POP (δ –19.9 ppm) and $[\text{Cu}(\text{POP})_2]^+$ (δ –13.6 ppm)^{11,32} were observed, most noticeably for $[\text{Cu}(\text{tpy})(\text{POP})][\text{PF}_6]$, $[\text{Cu}(1)(\text{POP})][\text{PF}_6]$, $[\text{Cu}(3)(\text{POP})][\text{PF}_6]$

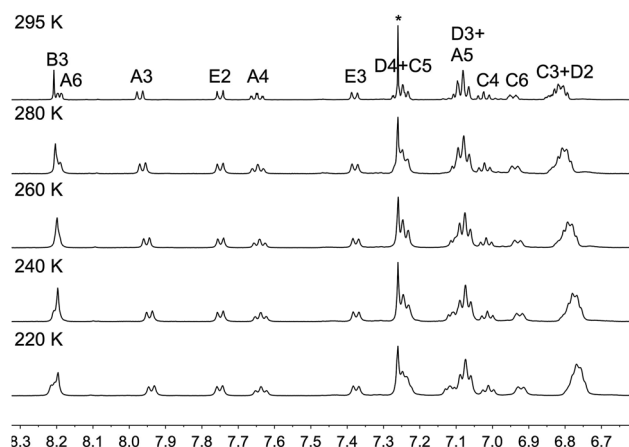


Fig. 2 Variable temperature 500 MHz ^1H NMR spectra of $[\text{Cu}(2)(\text{POP})][\text{PF}_6]$ (in CDCl_3 ; aromatic region only). Chemical shifts in δ/ppm . * = residual CHCl_3 .

and $[\text{Cu}(4)(\text{POP})][\text{PF}_6]$. A colourless, sometimes slightly blue, precipitate was also observed in the NMR tubes suggesting the formation of a copper(ii) species. For an NMR sample of $[\text{Cu}(3)(\text{POP})][\text{PF}_6]$, the CD_2Cl_2 was decanted off and the wet precipitate was dried and redissolved in a mixture of MeCN and MeOH, and was analysed by electrospray mass spectrometry. Dominant peak envelopes at m/z 601.3 and 368.2 were assigned to $[\text{Cu}(\text{POP})]^+$ (calc. m/z 601.1) and $[\text{3} + \text{H}]^+$ (calc. m/z 368.2); peak separation for each envelope was consistent with a singly charged ion. The third most intense peak envelope at m/z 398.8 with half-mass peak separation was assigned to $[\text{Cu}_3]^{2+}$ (calc. m/z 398.6). These observations indicate that the $[\text{Cu}(\text{tpy})(\text{POP})]^+$ complexes are less stable with respect to dissociation of POP and oxidation of copper(i) than $[\text{Cu}(\text{N}^{\wedge}\text{N})(\text{POP})]^+$ complexes in which $\text{N}^{\wedge}\text{N}$ is a bpy-containing ligand.^{2,6} The emission behaviour (see later) of the complexes also provides evidence for ligand dissociation in solution.

Single crystal structures of $[\text{Cu}(\text{tpy})(\text{POP})][\text{PF}_6]$ and $[\text{Cu}(4)(\text{POP})][\text{PF}_6]$

Single crystals of $[\text{Cu}(\text{tpy})(\text{POP})][\text{PF}_6]$ and $[\text{Cu}(4)(\text{POP})][\text{PF}_6]$ were grown from CH_2Cl_2 solutions of the respective complex layered with Et_2O . Both compounds crystallize in the monoclinic space group $P2_1/n$. The asymmetric unit of $[\text{Cu}(\text{tpy})(\text{POP})][\text{PF}_6]$ contains two independent cations Fig. 3. Table 1 lists pertinent bond parameters in the coordination spheres of the two independent Cu atoms, and Fig. 4 presents an overlay of the two cations. The conformations of the POP ligands are very similar, and the positions of the two central pyridine rings (Fig. 4, right) are approximately superimposed. In both cations, the P–Cu–P bite angle of the POP ligand is $\approx 121^\circ$ (Table 1). In the two independent cations, the shortest Cu– N_{tpy} bond involves the central pyridine ring, as expected for $\{\text{M}(\text{tpy})\}^{n+}$ domain.³³ These distances of 2.0901(11) and 2.0923(11) Å (Table 1) are similar to those observed for the Cu– $\text{N}_{\text{central-py}}$ distances in $[\text{Cu}(\text{tpy})(\text{PPh}_3)_2][\text{ClO}_4]$ (2.102(3) Å),¹⁸ and

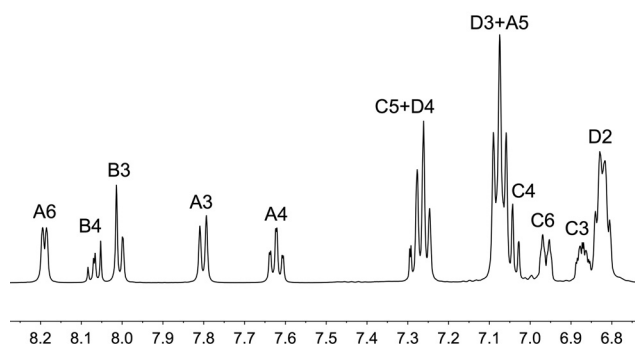


Fig. 1 500 MHz ^1H NMR spectrum of $[\text{Cu}(\text{tpy})(\text{POP})][\text{PF}_6]$ (295 K, CD_2Cl_2); see Scheme 2 for atom labelling. Chemical shifts in δ/ppm .



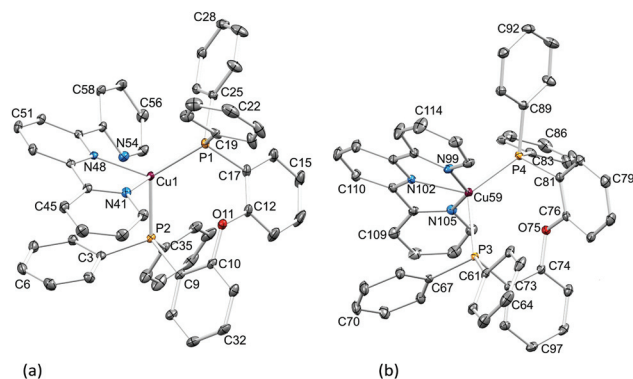


Fig. 3 The two independent cations in $[\text{Cu}(\text{tpy})(\text{POP})][\text{PF}_6]$ containing (a) 4-coordinate Cu1 and (b) 5-coordinate Cu59 (see text). Ellipsoids are plotted at 30% probability, and H atoms omitted for clarity.

Table 1 Selected bond parameters within the coordination spheres of Cu1 and Cu59 in the two independent $[\text{Cu}(\text{tpy})(\text{POP})]^+$ cations

Cation A			
Bond	Distance/Å	Bond angle	Angle/°
Cu1–N41	2.1117(11)	N41–Cu1–N48	79.78(4)
Cu1–N48	2.0901(11)	N48–Cu1–N54	63.15(4)
Cu1–N54	3.146(1)	P1–Cu1–P2	121.334(15)
Cu1–P1	2.2190(4)	N41–Cu1–P1	110.28(3)
Cu1–P2	2.3001(4)	N48–Cu1–P1	129.54(3)
		N41–Cu1–P2	94.10(3)
		N48–Cu1–P2	106.31(3)
Cation B			
Cu59–N99	2.2310(12)	N99–Cu59–N102	76.56(4)
Cu59–N102	2.0923(11)	N102–Cu59–N105	70.62(4)
Cu59–N105	2.6021(12)	P3–Cu59–P4	121.782(15)
Cu59–P3	2.2925(4)	N99–Cu59–P4	104.54(3)
Cu59–P4	2.2725(4)	N102–Cu59–P4	125.21(3)
		N99–Cu59–P3	106.09(3)
		N102–Cu59–P3	109.48(3)

$[\text{Cu}\{4'-(2\text{-Br-5-py})\text{tpy}\}(\text{PPh}_3)_2][\text{BF}_4]$ (2.121(3) Å).²⁰ In both cations, one of the Cu–N_{outer-py} distances is significantly shorter than the second. In cation A (Fig. 3a), the tpy domain is bidentate. Atom N54 of the non-coordinated pyridine ring faces towards the copper atom; analysing the thermal ellipsoids in both possible orientations of the pyridine ring (*i.e.* exchanging positions of N54 and C58, Fig. 3a) showed unambiguously that the chosen ring orientation was correct. The non-bonded separation Cu1–N54 is 3.146(1) Å and is associated with this pyridine ring being twisted 40.6° with respect to the central pyridine ring (Fig. 4). These structural features are similar to those observed in $[\text{Cu}\{4'-(2\text{-Br-5-py})\text{tpy}\}(\text{PPh}_3)_2]^+$.²⁰ The coordinated pyridine ring containing N41 is tilted through 27.5° with respect to the Cu–N bond vector, a feature that we have discussed in $[\text{Cu}(\text{bpy})(\text{POP})]^+$ complexes.⁶ In cation B, the two Cu–N_{outer-py} distances are 2.2310(12) and 2.6021(12) Å (Table 1). Although the latter is longer than a typical Cu–N

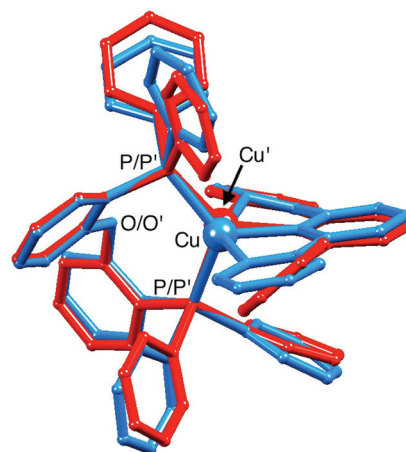


Fig. 4 Overlay of the structures of the two independent cations in $[\text{Cu}(\text{tpy})(\text{POP})][\text{PF}_6]$. One cation needs to be inverted before creating the overlay by matching the phosphorus atoms and the oxygen atom of each of the two POP ligands.

bond length, the values are similar to the corresponding bond distances in $[\text{Cu}(\text{tpy})(\text{PPh}_3)_2][\text{ClO}_4]^{18}$ in which the tpy is considered to be tridentate with the outer pyridine N-donors occupying the axial sites of a trigonal bipyramidal structure. The lattice of $[\text{Cu}(\text{tpy})(\text{POP})][\text{PF}_6]$ contains two independent $[\text{PF}_6]^-$ ions, one disordered; this has been modelled over two sites of occupancies of 90 and 10%.

Fig. 5 depicts the structure of the $[\text{Cu}(4)(\text{POP})]^+$ cation in $[\text{Cu}(4)(\text{POP})][\text{PF}_6]$; bond lengths and angles in the coordination sphere are given in the caption. The P2–Cu1–P18 angle of 115.07(5)° is smaller than those in the independent cations in $[\text{Cu}(\text{tpy})(\text{POP})][\text{PF}_6]$ (Table 1). Ligand 4 coordinates in a bidentate mode, and the rings comprising the coordinated bpy-domain are mutually twisted by 15.8°. The non-coordinated pyridine ring (with N65) is twisted 29.7° with respect to the

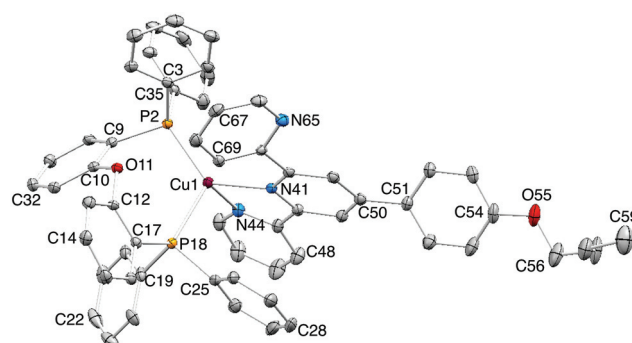


Fig. 5 Structure of the $[\text{Cu}(4)(\text{POP})]^+$ cation in $[\text{Cu}(4)(\text{POP})][\text{PF}_6]$; ellipsoids are plotted at 30% probability, and H atoms omitted for clarity. Important bond parameters: Cu1–P2 = 2.2316(13), Cu1–P18 = 2.3341(13), Cu1–N41 = 2.106(4), Cu1–N44 = 2.094(4) Å; P2–Cu1–P18 = 115.07(5), P2–Cu1–N41 = 128.90(11), P18–Cu1–N41 = 104.97(10), P2–Cu1–N44 = 121.04(12), P18–Cu1–N44 = 98.89(12), N41–Cu1–N44 = 80.12(15)°.



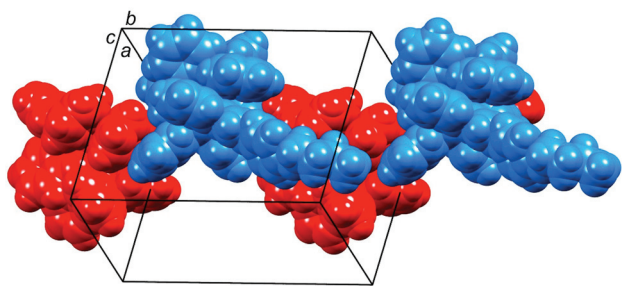


Fig. 6 Packing of cations in $[\text{Cu}(\mathbf{4})(\text{POP})][\text{PF}_6]$ along the b -axis.

ring containing atom N41 (Fig. 5) and atom N65 faces away from Cu1. This contrasts with the conformation of the non-coordinated pyridine ring in cation B in $[\text{Cu}(\text{tpy})(\text{POP})][\text{PF}_6]$ (Fig. 3b) and in $[\text{Cu}(\text{tpy})(\text{PPh}_3)_2][\text{ClO}_4]$.¹⁸ The correct orientation of the ring with N65 was confirmed by examination of the thermal ellipsoids of N65 and C69 when their positions were exchanged. The preference for this orientation may arise from a close inter-cation $\text{N}\cdots\text{H}-\text{C}_{\text{phenyl}}$ contact ($\text{N65}\cdots\text{H341}^{\text{i}}\text{C34}^{\text{i}} = 2.66 \text{ \AA}$; $\text{N65}\cdots\text{H341}^{\text{i}}-\text{C34}^{\text{i}} = 134^\circ$). Propagation of these interactions results in the formation of chains of cations along the b -axis (Fig. 6); each extended n -butoxy substituent embraces an adjacent cation.

Photophysical properties

The solution absorption spectra of $[\text{Cu}(\text{N}^{\wedge}\text{N})(\text{POP})][\text{PF}_6]$ ($\text{N}^{\wedge}\text{N} = \text{tpy}, \mathbf{1}-\mathbf{4}$) are shown in Fig. 7. In each complex cation, $\pi^* \leftarrow \pi$ and $\pi^* \leftarrow n$ transitions³⁴ give rise to an intense high energy band at $\approx 230 \text{ nm}$ and broader absorptions in the 270–330 nm range. The spectra of $[\text{Cu}(\text{tpy})(\text{POP})][\text{PF}_6]$ and $[\text{Cu}(\mathbf{1})(\text{POP})][\text{PF}_6]$ are similar, consistent with these complexes differing only in the introduction of two methyl substituents on going from tpy to **1**. Enhancement of the absorption band at 282 nm on going from $[\text{Cu}(\text{tpy})(\text{POP})][\text{PF}_6]$ to $[\text{Cu}(\mathbf{2})(\text{POP})][\text{PF}_6]$ follows from the introduction of the tolyl group in **2**. Similarities between the UV regions of the absorption spectra of $[\text{Cu}(\mathbf{3})(\text{POP})][\text{PF}_6]$ and $[\text{Cu}(\mathbf{4})(\text{POP})][\text{PF}_6]$ and their relatively intense bands at

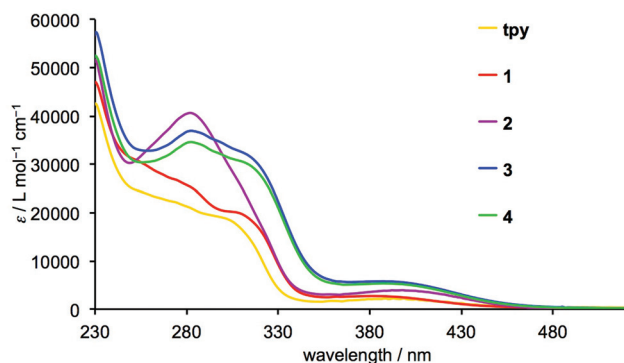


Fig. 7 Solution absorption spectra of $[\text{Cu}(\text{N}^{\wedge}\text{N})(\text{POP})][\text{PF}_6]$ for $\text{N}^{\wedge}\text{N} = \text{tpy}, \mathbf{1}-\mathbf{4}$. (CH_2Cl_2 , $2.5 \times 10^{-5} \text{ mol dm}^{-3}$).

$ca. 280\text{--}320 \text{ nm}$ are consistent with the extended π -conjugation in ligands **3** and **4** compared to tpy. All the complexes exhibit a low intensity metal-to-ligand charge transfer (MLCT) band at $ca. 390 \text{ nm}$, which is at a similar energy to those observed for $[\text{Cu}(\text{bpy})(\text{POP})]^+$, $[\text{Cu}(\text{6-Mebpy})(\text{POP})]^+$, $[\text{Cu}(\text{6,6'-Me}_2\text{bpy})(\text{POP})]^+$, $[\text{Cu}(\text{phen})(\text{POP})]^+$ and $[\text{Cu}(\text{2,9-Me}_2\text{phen})(\text{POP})]^+$,^{2,6,13,35} (6-Mebpy = 6-methyl-2,2'-bipyridine; 6,6'-Me₂bpy = 6,6'-dimethyl-2,2'-bipyridine; 2,9-Me₂phen = 2,9-dimethyl-1,10-phenanthroline).

In the solid state, the complexes are all weakly emissive when excited at 365 nm. Emission bands are broad and without structure (Fig. 8). Since X-ray diffraction studies have revealed differing coordination modes of the tpy domain in the solid state, it is difficult to say anything about the trend in values of the emission maxima. However, the range of $\lambda_{\text{em}}^{\text{max}}$ values (535 to 589 nm, Table 2) is consistent with $\lambda_{\text{em}}^{\text{max}}$ for solid $[\text{Cu}(\text{6-Mebpy})(\text{POP})][\text{PF}_6]$ (567 nm) and $[\text{Cu}(\text{6,6'-Me}_2\text{bpy})(\text{POP})][\text{PF}_6]$ (535 nm).⁶ The photoluminescence quantum yields of the tpy-containing $[\text{Cu}(\text{N}^{\wedge}\text{N})(\text{POP})][\text{PF}_6]$ complexes are very low and the emission lifetimes all around 1 μs (Table 2).

Dichloromethane solutions of $[\text{Cu}(\text{N}^{\wedge}\text{N})(\text{POP})][\text{PF}_6]$ with $\text{N}^{\wedge}\text{N} = \text{tpy}$ or **1–4** were very poorly emissive at room temperature and, where observed, emission maxima were blue-shifted with respect to those recorded for powder samples. As an example, Fig. 9 shows the normalized powder and solution spectra for $[\text{Cu}(\mathbf{1})(\text{POP})][\text{PF}_6]$. This shift to higher energy is not consistent with the trend observed for $[\text{Cu}(\text{6-Mebpy})(\text{POP})]^+$,⁶

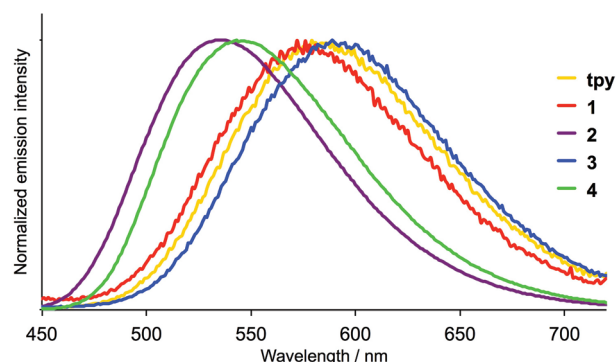


Fig. 8 Normalized emission spectra of powdered $[\text{Cu}(\text{N}^{\wedge}\text{N})(\text{POP})][\text{PF}_6]$ for $\text{N}^{\wedge}\text{N} = \text{tpy}, \mathbf{1}-\mathbf{4}$.

Table 2 Emission maxima,^a photoluminescence quantum yields and lifetimes for powdered samples of $[\text{Cu}(\text{N}^{\wedge}\text{N})(\text{POP})][\text{PF}_6]$

Complex cation	$\lambda_{\text{em}}^{\text{max}}/\text{nm}$	$\tau/\mu\text{s}$	PLQY/%
$[\text{Cu}(\text{tpy})(\text{POP})]^+$	582	1.12	0.8
$[\text{Cu}(\mathbf{1})(\text{POP})]^+$	573	1.07	0.6
$[\text{Cu}(\mathbf{2})(\text{POP})]^+$	535	1.88	1.0
$[\text{Cu}(\mathbf{3})(\text{POP})]^+$	589	1.18	0.7
$[\text{Cu}(\mathbf{4})(\text{POP})]^+$	542	1.10	0.8

^a $\lambda_{\text{exc}} = 365 \text{ nm}$.



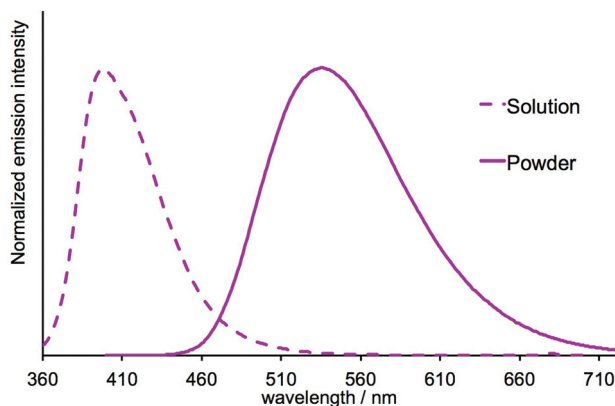


Fig. 9 Normalized emission spectra for solid $[\text{Cu}(\mathbf{1})(\text{POP})][\text{PF}_6]$ ($\lambda_{\text{exc}} = 365 \text{ nm}$) and for a CH_2Cl_2 solution of $[\text{Cu}(\mathbf{1})(\text{POP})][\text{PF}_6]$ ($\lambda_{\text{exc}} = 340 \text{ nm}$); the emission in solution probably arises from $\mathbf{1}$ or $[\text{H}\mathbf{1}]^+$ (see text).

$[\text{Cu}(6,6'\text{-Me}_2\text{bpy})(\text{POP})]^+$,⁶ $[\text{Cu}(\text{POP})(\text{pypz})]^+$,¹⁰ and $[\text{Cu}(\text{POP})(3\text{-Mepypz})]^+$,¹⁰ (pypz = 2-pyridylpyrazole, 3-Mepypz = 3-methyl-2-pyridylpyrazole) where a significant red-shift in $\lambda_{\text{em}}^{\text{max}}$ occurs on going from solid to solution. The emission at 396 nm for $[\text{Cu}(\mathbf{1})(\text{POP})][\text{PF}_6]$ in solution (Fig. 9) is close to that observed for free $\mathbf{1}$,³⁶ and the observed spectrum most probably arises from $\mathbf{1}$ or protonated ligand^{36,37} rather than the copper(i) complex. It is well established that in solution (both in coordinating and non-coordinating solvents) tetrahedral copper(i) complexes undergo exciplex formation leading to solvent quenching of the emission.^{38,39} The solution spectra of $[\text{Cu}(\text{N}^{\wedge}\text{N})(\text{POP})][\text{PF}_6]$ with $\text{N}^{\wedge}\text{N} = \text{tpy}$ or $\mathbf{1-4}$ are therefore easily dominated by emissions arising from dissociation products, even if present only in small amounts. A CH_2Cl_2 solution of $[\text{Cu}(\text{tpy})(\text{POP})][\text{PF}_6]$ excited at 340 nm exhibited broad emissions with $\lambda_{\text{em}}^{\text{max}} = 438 \text{ nm}$ and 502 nm. The former is close to that reported for free POP ($\lambda_{\text{em}}^{\text{max}} = 430 \text{ nm}$ in air-free THF at room temperature).³² These data are consistent with the NMR spectroscopic evidence for ligand dissociation discussed earlier.

The complex $[\text{Cu}(\mathbf{4})(\text{POP})][\text{PF}_6]$ was employed in preliminary tests in a LEC device configuration⁴⁰ but did not exhibit electroluminescence.

Conclusions

We have prepared and characterized the first examples of $[\text{Cu}(\text{N}^{\wedge}\text{N})(\text{POP})]^+$ complexes in which the $\text{N}^{\wedge}\text{N}$ domain is a 2,2':6',2''-terpyridine ligand. Single crystal X-ray diffraction data confirm that 2,2':6',2''-terpyridines can function in this type of copper(i) complex as bidentate or tridentate ligands. However, the structural data suggest that the energy difference between different modes of coordination are small and are easily tipped by packing interactions. In solution, the tpy domain is C_2 -symmetric even at low temperature, consistent with either tridentate coordination or a low energy dynamic process involving bidentate ligands. In contrast to $[\text{Cu}(\text{N}^{\wedge}\text{N})-$

$(\text{POP})]^+$ complexes in which $\text{N}^{\wedge}\text{N}$ is bpy or phen-based, those with tpy ligands are less stable with respect to ligand dissociation and oxidation of copper(i). $[\text{Cu}(\text{N}^{\wedge}\text{N})(\text{POP})]^+$ complexes with $\text{N}^{\wedge}\text{N} = \text{tpy}$ or $\mathbf{1-4}$ are poorly emissive in the solid state at room temperature, and in solution, emission behaviour is consistent with ligand dissociation. We conclude that members of this family of compounds, while structurally interesting, are not promising candidates for LECs.

Acknowledgements

We thank the European Research Council (Advanced Grant 267816 LiLo), Swiss National Science Foundation (200020_144500), the European Union (CELLO, STRP 248043) and the University of Basel for financial support. Dr Jonas Schönle is thanked for the syntheses of $\mathbf{1}$ and $\mathbf{2}$. Dr Henk J. Bolink and Antonio Pertegás, Instituto de Ciencia Molecular, Universidad de Valencia are acknowledged for preliminary LEC device testing.

Notes and references

- R. D. Costa, E. Ortí, H. J. Bolink, F. Monti, G. Accorsi and N. Armaroli, *Angew. Chem., Int. Ed.*, 2012, **51**, 8178.
- R. D. Costa, D. Tordera, E. Ortí, H. J. Bolink, J. Schönle, S. Graber, C. E. Housecroft, E. C. Constable and J. A. Zampese, *J. Mater. Chem.*, 2011, **21**, 16108.
- N. Armaroli, G. Accorsi, M. Holler, O. Moudam, J. F. Nierengarten, Z. Zhou, R. T. Wegh and R. Welter, *Adv. Mater.*, 2006, **18**, 1313.
- O. Moudam, A. Kaeser, B. Delavaux-Nicot, C. Duhayon, M. Holler, G. Accorsi, N. Armaroli, I. Seguy, J. Navarro, P. Destruel and J. F. Nierengarten, *Chem. Commun.*, 2007, 3077.
- J.-J. Cid, J. Mohanraj, M. Mohankumar, M. Holler, F. Monti, G. Accorsi, L. Karmazin-Brelot, I. Nierengarten, J. M. Malicka, M. Cocchi, B. Delavaux-Nicot, N. Armaroli and J. F. Nierengarten, *Polyhedron*, 2014, **82**, 158 and references therein.
- S. Keller, E. C. Constable, C. E. Housecroft, M. Neuburger, A. Prescimone, G. Longo, A. Pertegás, M. Sessolo and H. J. Bolink, *Dalton Trans.*, 2014, **43**, 16593.
- K. Zhang and D. Zhang, *Spectrochim. Acta, Part A*, 2013, **124**, 341.
- L. Bergmann, J. Friedrichs, M. Mydlak, T. Baumann, M. Nieger and S. Bräse, *Chem. Commun.*, 2013, **49**, 6501.
- E. Mejía, S.-P. Luo, M. Karnahl, A. Friedrich, S. Tschierlei, A.-E. Surkus, H. Junge, S. Gladiali, S. Lochbrunner and M. Beller, *Chem. – Eur. J.*, 2013, **19**, 15972.
- X.-L. Chen, R. Yu, Q.-K. Zhang, L.-J. Zhou, X.-Y. Wu, Q. Zhang and C.-Z. Lu, *Chem. Mater.*, 2013, **25**, 3910.
- A. Kaeser, M. Mohankumar, J. Mohanraj, F. Monti, M. Holler, J.-J. Cid, O. Moudam, I. Nierengarten,



- L. Karmazin-Brelot, C. Duhayon, B. Delavaux-Nicot, N. Armaroli and J.-F. Nierengarten, *Inorg. Chem.*, 2013, **52**, 12140.
- 12 C. Femoni, S. Muzzioli, A. Palazzi, S. Stagni, S. Zacchini, F. Monti, G. Accorsi, M. Bolognesi, N. Armaroli, M. Massi, G. Valenti and M. Marcaccio, *Dalton Trans.*, 2013, **42**, 997.
 - 13 I. Andrés-Tomé, J. Fyson, F. Baiao Dias, A. P. Monkman, G. Iacobellis and P. Coppo, *Dalton Trans.*, 2012, **41**, 8669.
 - 14 C. L. Linfoot, M. J. Leidl, P. Richardson, A. F. Rausch, O. Chepelin, F. J. White, H. Yersin and N. Robertson, *Inorg. Chem.*, 2014, **53**, 10854.
 - 15 E. C. Constable, C. E. Housecroft, G. E. Schneider, J. A. Zampese, H. J. Bolink, A. Pertegás and C. Roldan-Carmona, *Dalton Trans.*, 2014, **43**, 4653.
 - 16 F. Kröhnke, *Synthesis*, 1976, 1.
 - 17 J. Wang and G. S. Hanan, *Synlett*, 2005, 1251.
 - 18 E. W. Ainscough, A. M. Brodie, S. L. Ingham and J. M. Waters, *J. Chem. Soc., Dalton Trans.*, 1994, 215.
 - 19 Q. Feng, D. Li, Y.-G. Yin, X.-L. Feng and J.-W. Cai, *Huaxue Xuebao*, 2002, **60**, 2167.
 - 20 M. I. J. Polson, G. S. Hana and N. J. Taylor, *Acta Crystallogr., Sect. E: Struct. Rep. Online*, 2008, **64**, m205.
 - 21 D. L. Jameson and L. E. Guise, *Tetrahedron Lett.*, 1991, **32**, 1999.
 - 22 A. Livoreil, C. O. Dietrich-Buchecker and J.-P. Sauvage, *J. Am. Chem. Soc.*, 1994, **116**, 9399.
 - 23 B. Tang, F. Yu, P. Li, L. Tong, X. Duan, T. Xie and X. Wang, *J. Am. Chem. Soc.*, 2009, **131**, 3016.
 - 24 Y. M. Klein, E. C. Constable, C. E. Housecroft, J. A. Zampese and A. Crochet, *CrystEngComm*, 2014, **16**, 9915.
 - 25 G. J. Kubas, *Inorg. Synth.*, 1979, **19**, 90.
 - 26 APEX2, version 2 User Manual, Bruker Analytical X-ray Systems, Inc., M86-E01078, Madison, WI, 2006.
 - 27 P. W. Betteridge, J. R. Carruthers, R. I. Cooper, K. Prout and D. J. Watkin, *J. Appl. Crystallogr.*, 2003, **36**, 1487.
 - 28 I. J. Bruno, J. C. Cole, P. R. Edgington, M. K. Kessler, C. F. Macrae, P. McCabe, J. Pearson and R. Taylor, *Acta Crystallogr., Sect. B: Struct. Sci.*, 2002, **58**, 389.
 - 29 C. F. Macrae, I. J. Bruno, J. A. Chisholm, P. R. Edgington, P. McCabe, E. Pidcock, L. Rodriguez-Monge, R. Taylor, J. van de Streek and P. A. Wood, *J. Appl. Crystallogr.*, 2008, **41**, 466.
 - 30 C. L. Linfoot, P. Richardson, T. E. Hewat, O. Moudam, M. M. Forde, A. Collins, F. White and N. Robertson, *Dalton Trans.*, 2010, **39**, 8945.
 - 31 E. C. Constable, A. J. Edwards, M. J. Hannon and P. R. Raithby, *J. Chem. Soc., Chem. Commun.*, 1994, 1991; G. Baum, E. C. Constable, D. Fenske, C. E. Housecroft, T. Kulke, M. Neuburger and M. Zehnder, *J. Chem. Soc., Dalton Trans.*, 2000, 945; C.-T. Yeung, H.-L. Yeung, C.-S. Tsang, W.-Y. Wong and H.-L. Kwong, *Chem. Commun.*, 2007, 5203.
 - 32 A. Kaeser, O. Moudam, G. Accorsi, I. Séguy, J. Navarro, A. Belbakra, C. Duhayon, N. Armaroli, B. Delavaux-Nicot and J.-F. Nierengarten, *Eur. J. Inorg. Chem.*, 2014, 1345.
 - 33 E. C. Constable, *Adv. Inorg. Chem. Radiochem.*, 1986, **30**, 69.
 - 34 N. Armaroli, G. Accorsi, F. Cardinali and A. Listorti, *Top. Curr. Chem.*, 2007, **280**, 69.
 - 35 K. Zhang and D. Zhang, *Spectrochim. Acta, Part A*, 2013, **124**, 341.
 - 36 N. Yoshikawa, S. Yamabe, N. Kanehisa, T. Inoue, H. Takashima and K. Tsukahara, *J. Phys. Org. Chem.*, 2010, **23**, 431.
 - 37 N. Yoshikawa, S. Yamabe, N. Kanehisa, H. Takashima and K. Tsukahara, *J. Phys. Org. Chem.*, 2009, **22**, 410.
 - 38 D. R. McMillin, J. R. Kirchhoff and K. V. Goodwin, *Coord. Chem. Rev.*, 1985, **64**, 83.
 - 39 N. A. Gothard, M. W. Mara, J. Huang, J. M. Szarko, B. Rolczynski, J. V. Lockard and L. X. Chen, *J. Phys. Chem. A*, 2012, **116**, 1984.
 - 40 R. D. Costa, D. Tordera, E. Ortí, H. J. Bolink, J. Schönle, S. Graber, C. E. Housecroft, E. C. Constable and J. A. Zampese, *J. Mater. Chem.*, 2011, **21**, 16108.

